Topology of the substrate-binding site of a Lys^{49}-phospholipase A_2 influences Ca^{2+}-independent membrane-damaging activity

Juliana Martha SÁ*, Lucimara CHIOATO*, Tatiana Lopes FERREIRA†, Arthur H. C. DE OLIVEIRA‡, Roberto RULLER‡, José César ROSA‡§, Lewis J. GREENE‡§ and Richard J. WARD†[1]

*Departamento de Bioquímica e Immunologia, FMRP-USP, Ribeirão Preto-SP, Brazil, †Departamento de Química, FFCLRP-USP, Avenida Bandeirantes 3900, CEP 14049-901, Ribeirão Preto-SP, Brazil, ‡Departamento de Biologia Molecular e Celular e Bioagentes Patogênicos, FMRP-USP, Universidade de São Paulo, Ribeirão Preto-SP, Brazil, and §Centro de Química de Proteínas, FMRP-USP, Universidade de São Paulo, Ribeirão Preto-SP, Brazil

BthTx-I (bothropstoxin-I) is a myotoxic Lys^{49}-PLA_2 (phospholipase A_2 with Lys^{49}) isolated from *Bothrops jararacussu* venom, which damages liposome membranes by a Ca^{2+}-independent mechanism. The highly conserved Phe^5/Ala^{102}/Phe^{106} motif in the hydrophobic substrate-binding site of the Asp^{49}-PLA_2s is substituted by Leu^5/Val^{102}/Leu^{106} in the Lys^{49}-PLA_2s. The Leu^5/Val^{102}/Leu^{106} triad in BthTx-I was sequentially mutated via all single- and double-mutant combinations to the Phe^5/Ala^{102}/Phe^{106} mutant. All mutants were expressed as inclusion bodies in *Escherichia coli*, and the thermal stability (T_m), together with the myotoxic and Ca^{2+}-independent membrane-damaging activities of the recombinant proteins, were evaluated. The far-UV CD profiles of the native, wild-type recombinant and the L106F (Leu^{106} → Phe) and L5F/F102A/L106F mutant proteins were identical. The L5F, V102A, L5F/V102A and V102A/L106F mutants showed distorted far-UV CD profiles; however, only the L5F and L5F/V102A mutants showed significant decreases in T_m. Alterations in the far-UV CD spectra correlated with decreased myotoxicity and protein-induced release of a liposome-entrapped marker. However, the V102A/L106F and L5F/V102A/L106F mutants, which presented high myotoxic activities, showed significantly reduced membrane-damaging activity. This demonstrates that the topology of the substrate-binding region of BthTx-I has a direct effect on the Ca^{2+}-independent membrane damage, and implies that substrate binding retains an important role in this process.

Key words: bothropstoxin-I, Lys^{49}-phospholipase A_2 (Lys^{49}-PLA_2), mutagenesis, myotoxicity, substrate-binding site, topology.

INTRODUCTION

Phospholipases A_2 (PLA_2s; EC 3.1.1.4) catalyse the hydrolysis of the *sn*-2 acyl bonds of *sn*-3 phospholipids [1], and are currently classified into 11 groups on the basis of amino acid sequence similarity [2]. The hydrolysis of phospholipids by group I/II PLA_2s involves a His^{48}/Asp^{99} pair in the catalytic site, which activates a positionally conserved water molecule, thereby initiating the nucleophilic attack on the *sn*-2 position of the substrate. A Ca^{2+} ion cofactor is bound to the carboxyl oxygen atoms of Asp^{49} and carbonyl main-chain oxygens of the neighbouring calcium-binding loop stabilizes the tetrahedral intermediate during catalysis [3,4].

A subfamily of class IIB PLA_2s in which Asp^{49} is substituted by a lysine residue have been identified in several Asiatic and new world Viperid snake venoms (see [5–7] for reviews). Initial reports suggested that these Lys^{49}-PLA_2s (PLA_2s with Lys^{49}) retained low levels of catalytic activity [8–10]; however, subsequent studies with both native [11–13] and recombinant [14] proteins have failed to detect hydrolysis of phospholipid substrates. The crystal structures of Lys^{49}-PLA_2s have demonstrated that the ε-amino group of the Lys^{49} is located in the position occupied by Ca^{2+} in Asp^{49}-PLA_2s [4,14,15], and it has been suggested that the reduction or elimination of catalytic activity results from either the reorientation of the Cys^{29}–Gly^{30} peptide bond [14] or the reduced binding affinity of the Ca^{2+} cofactor [16]. Despite the absence of detectable catalytic activity, the Lys^{49}-PLA_2s demonstrate membrane-damaging activity through a Ca^{2+}-independent, non-hydrolytic mechanism [17–19].

Bothropstoxin-I (referred to as BthTx-I) is a Lys^{49}-PLA_2 isolated from the venom of *Bothrops jararacussu*, which forms homodimers both in solution [19] and in the crystalline state [20]. Flexibility at the dimer interface permits a quaternary structure transition between 'open' and 'closed' forms, and it has been proposed that, in the membrane-bound form, this transition may disrupt the packing of the bilayer lipid, thereby resulting in disruption of the membrane [20]. The model predicts that, as a result of the conformational transition, the position of the C-terminal loop region of the protein is altered, which promotes a more intimate interaction of this region with the membrane bilayer. Indeed, site-directed mutagenesis has demonstrated that residues in the C-terminal loop region play an important role in the Ca^{2+}-independent membrane-damaging activity [21].

Comparison of the Lys^{49}-PLA_2 amino acid sequences with those of the Asp^{49}-PLA_2s has revealed that amino acid substitutions that are specific to the Lys^{49}-PLA_2s are grouped in three distinct clusters in the crystal structure [22]. In addition to residue clusters in the β-wing and active-site regions, the highly conserved Phe^5/Ala^{102}/Phe^{106} triad in the hydrophobic substrate-binding cleft of the Asp^{49}-PLA_2s is substituted by Leu^5/Val^{102}/Leu^{106} in the Lys^{49}-PLA_2s [22,23]. Previously, it has been demonstrated that the catalytic activity of the Asp^{49}-PLA_2s is highly sensitive to site-directed mutagenesis of these residues [24,25], and therefore, the changes observed in the substrate-binding region of the Lys^{49}-PLA_2s are particularly intriguing. This cluster of amino acid substitutions results in a significant alteration in the topology of the substrate-binding region; however, it is tolerated in the sense that the product is a biologically functional (although catalytically

Abbreviations used: CK, creatine kinase; PLA_2, phospholipase A_2; Lys^{49}-PLA_2, phospholipase A_2 with Lys^{49}; BthTx-I, bothropstoxin-I; EYPC, egg yolk phosphatidylcholine.

[1] To whom correspondence should be addressed (email rjward@fmrp.usp.br).

inactive) protein. The effects of substituting the highly conserved Phe[5]/Ala[102]/Phe[106] triad in the Lys[49]-PLA_2s are not known, and to understand the effects of these specific substitutions in the substrate-binding region of the Lys[49]-PLA_2s, we have sequentially mutated the Leu[5]/Val[102]/Leu[106] residues to the Phe[5]/Ala[102]/Phe[106] residues encountered in the Asp[49]-PLA_2s. The effects of these mutations were evaluated using several structural and functional assays, which have revealed that the topology of the substrate-binding region influences the calcium-independent membrane-damaging activity, and suggest a functional linkage between the substrate-binding and C-terminal loop regions.

EXPERIMENTAL

Native protein purification and sample preparation

BthTx-I was purified from crude freeze-dried *B. jararacussu* venom using cation-exchange chromatography as described previously [26]. Protein purity was routinely evaluated by silver staining of SDS/polyacrylamide gels, and aliquots of the purified protein were stored at − 20 °C until further use.

Site-directed mutagenesis

A full-length cDNA encoding BthTx-I has been isolated previously from *B. jararacussu* venom gland cDNA by reverse transcriptase–PCR [27] (GenBank® accession no. X78599), and subcloned into the expression vector pET3-d [28]. Nucleotide sequencing has confirmed the construct in which Ser[1] of the BthTx-I is preceded by a methionine residue, and a stop codon immediately follows Cys[133] (the homology numbering scheme reported by Heinrickson [29] is used throughout the present study). After linearization of this construct with *Sca*I, site-directed mutagenesis of the BthTx-I was performed by PCR mutagenesis [30] to introduce the following single mutations: L5F (oligonucleotide 5′-CATTTTCCCGAACTCAAACAG-3′; base changes are underlined), V102A (5′-GCAGATTGCCGCGGCCTTGTC-3′), L106F (5′-ATTTTCTCGGAAGCAGATTGC-3′) and L106F (5′-ATTTTCTCGGGCGCAGATTGC-3′). The double mutants L5F/V102A, L5F/L106F and V102A/L106F, together with the triple mutant L5F/V102A/L106F, were obtained by mutagenesis of the respective single- and double-mutant constructs. PCRs were performed using oligonucleotides complementary to the vector sequences flanking the BthTx-I insert, which contained restriction sites for *Xba*I (5′-extremity) and *Bam*HI (3′-extremity). After digestion with these enzymes, the amplified fragments were subcloned into the equivalent sites in the expression vector pET3d and fully sequenced.

Recombinant protein expression and purification

Growth medium (400 mg/l; 25 g of yeast extract, 15 g of tryptone, 10 mM $MgSO_4$, 35 μg of chloramphenicol and 100 μg of ampicillin, pH 7.5) was inoculated with the *Escherichia coli* strain BL21-(DE3){pLysS} transformed with the native or mutant constructs, and grown at 37 °C to an absorbance A_{600} 0.6. Recombinant protein expression was induced by the addition of 0.6 mM isopropyl β-D-thiogalactoside, and the culture was grown for an additional 7 h. Inclusion bodies were isolated from bacterial pellets by repeated rounds of sonication in 20 ml of lysis buffer (50 mM Tris/HCl, pH 8.0, 1 mM EDTA, 0.4 M urea and 1 % Triton X-100), followed by centrifugation at 12 000 ***g***. The method for the solubilization and refolding of recombinant BthTx-I in the presence of a gel-filtration medium was performed as described previously [28]. The refolded protein was purified by cation-exchange chromatography using a 100 mm × 7 mm column packed with Resource S resin (Amersham Biosciences, São Paulo, Brazil) previously equilibrated in 20 mM Tris/HCl, pH 8.0 (buffer A). After application of the sample, the column was eluted with buffer A supplemented with 1 M NaCl, and the absorbance of the eluate was monitored continuously at 280 nm. The eluted protein was dialysed against 5 mM Tris/HCl (pH 8.0) for 36 h with buffer changes every 12 h, and finally stored at 4 °C until further use.

MS analysis

Protein was diluted in 50 % (v/v) acetonitrile and 0.1 M ammonium bicarbonate and reduced with 45 mM dithiothreitol for 1 h at 56 °C, and subsequently alkylated with 100 mM iodoacetamide for 1 h at room temperature (25 °C) in the dark. The protein solution was diluted 5-fold and 0.5 μg of modified trypsin (Promega, Madison, WI, U.S.A.) was added; after 24 h, trypsin hydrolysis was stopped with 5 μl of formic acid. The tryptic peptides were desalted with Poros R2 (PerSeptive Biosystems, Hertford, U.K.) and eluted in 60 % (v/v) methanol and 5 % (v/v) formic acid, and MS analysis of tryptic peptides was performed in an electrospray triple-quadrupole mass spectrometer Quatro II (Micromass, Manchester, U.K.). The samples were infused using a syringe pump at a flow rate of 300 nl/min under the following conditions: capillary voltage was maintained at 2.8 kV, cone voltage at 40 V and cone temperature at 100 °C. The parameters for MS scanning were optimized with a synthetic peptide for the highest signal-to-noise ratio. The spectrum was collected as the average of 14–25 scans (2–5 s/scan) over the range 300–2000 atomic mass units, and processed using MassLynx software v.3.3 (Micromass). The site-directed mutant tryptic peptides were submitted to CID (collision-induced dissociation)–MS/MS to produce fragment ions type b and y, which were used to deduce the amino acid sequence. The collision cell was set to a collision energy of 20–25 eV for double-charged ions and 38–45 eV for single-charged ions, and argon was used as the collision gas at a pressure of 0.4 mPa (3.0×10^{-3} mTorr). Each spectrum was collected as the average of 13–20 (3 s/scan) and processed using MassLynx software.

CD spectroscopy

Far-UV CD spectra of BthTx-I and the mutants were measured between 200 and 250 nm in 20 mM Hepes (pH 7.0) at 25 °C with a JASCO J-810 spectropolarimeter (Jasco, Tokyo, Japan) using 1 mm path-length cuvettes and a protein concentration of 70–150 $\mu g \cdot ml^{-1}$ BthTx-I. In each case, a total of nine spectra were collected, averaged and corrected by subtraction of a buffer blank. Thermal denaturation studies were performed using the J-810 spectropolarimeter equipped with a Peltier-type temperature controller (PTC423S; Jasco) with a heating rate of 1 $°C \cdot min^{-1}$ using 1 cm path-length cuvettes and a protein concentration of 50–150 $\mu g \cdot ml^{-1}$. Changes in the ellipticity signal at 222 nm were monitored over the temperature range 30–90 °C (303.16–363.16 K). The melting temperature T_m was determined from the thermal denaturation curve by assuming a two-state mechanism and using a least-squares fitting routine derived from the van't Hoff equation as described previously [31].

Release of entrapped fluorescent markers from liposomes

Membrane damaging activity was determined by measuring the release of the liposome-entrapped, self-quenching fluorescent dye calcein. Loss of liposome membrane integrity results in dilution of the fluorophore, with a consequent increase in the fluorescence signal [18,19]. Liposomes composed of EYPC (egg yolk phosphatidylcholine)/DMPA (dimyristoyl phosphatidic acid) at a molar ratio of 9:1 were prepared by reverse-phase evaporation

with a buffer (25 mM Hepes and 150 mM NaCl, pH 7.0) containing 25 mM calcein (Sigma). The liposomes were passed through a 400 nm polycarbonate filter and applied to a Sephadex G50 column (1 cm × 8 cm) to separate the liposomes from the free calcein. Proteins and liposomes were mixed to a final protein/lipid molar ratio of 1:400, and the kinetics of membrane damage was monitored by the increase in fluorescence with emission at 520 nm and excitation at 490 nm, and the signal was expressed as percentage of total calcein release after the addition of 5 mM Triton X-100.

Myotoxic activity

Protein (30 μg) in a total volume of 50 μl of PBS was injected into the gastrocnemius muscle of male Swiss mice (weighing 18–22 g). After 3 h, a blood sample was collected from the tail in a heparinized capillary tube and the plasma was separated by centrifugation. The plasma CK (creatine kinase) activity was determined using 4 μl of plasma using the CK-UV kinetic kit (Sigma) according to the manufacturer's instructions. CK activity was expressed in terms of unit $\cdot$ l^{-1}, where 1 unit is defined as the amount of enzyme that produces 1 mmol of NADH $\cdot$ min^{-1} under the standard conditions used in the assay. Animals used as negative controls received 50 μl of PBS, and all results were expressed as the mean plasma CK activity from a minimum of five experiments.

Table 1 Results of MS analysis of the native and wild-type recombinant BthTx-I and mutant peptides

		Calculated mass†		Observed mass	
Mutant	Peptide sequence*	$[M+H^+]$	$[M+2H^+]$	$[M+H^+]$	$[M+2H^+]$
Native	S^{1}LFELGK^{7}	793.5	397.3	793.5	–
	A^{101}VAICLR^{107}	802.5	401.7	802.5	401.8
Recombinant	S^{1}LFELGK^{7}	793.5	397.3	793.4	–
	A^{101}VAICLR^{107}	802.5	401.7	802.4	401.8
L5F	S^{1}LFE**F**GK^{7}	827.9	414.2	827.5	–
V102A	A^{101}**A**AICLR^{107}	774.4	387.7	–	387.8
L106A	A^{101}VAIC**A**R^{107}	760.4	380.7	760.5	–
L106F	A^{101}VAIC**F**R^{107}	836.5	418.7	836.6	418.1
L5F/V102A	S^{1}LFE**F**GK^{7}	827.9	414.2	827.5	–
	A^{101}**A**AICLR^{107}	774.4	387.7	774.5	387.8
L5F/L106F	S^{1}LFE**F**GK^{7}	827.9	414.2	827.4	–
	A^{101}VAIC**F**R^{107}	836.5	418.7	–	418.9
V102A/L106F	A^{101}**A**AIC**F**R^{107}	808.4	404.7	–	404.2
L5F/V102A/L106F	S^{1}LFE**F**GK^{7}	827.9	414.2	827.5	414.3
	A^{101}**A**AIC**F**R^{107}	808.4	404.7	808.5	404.8

* Mutations from the native amino acid sequence are shown in boldface. The superscript numbers indicate the initial and final amino acid positions of the peptide according to the homology numbering scheme reported by Heinrickson [29].

† The mass of cysteine residue was calculated by modification to carboxyamidomethylcysteine.

RESULTS

As reported previously [28], BthTx-I is expressed in the form of inclusion bodies in *E. coli*, and all mutants were successfully expressed using this host cell (results not shown). After solubilization, chemical modification and refolding, the recombinant proteins were purified using cation-exchange chromatography, and assessment of purity by silver staining of SDS/polyacrylamide gels revealed a single protein band in all cases (results not shown). All proteins were exposed to trypsin digestion, and the resulting peptides corresponding to amino acids 1–7 (BthTx-I$^{1\text{-}7}$) and 101–107 (BthTx-I$^{101\text{-}107}$) were analysed using ESI (electrospray ionization)–MS. Table 1 demonstrates that these peptides present identical masses both in the native and wild-type recombinant proteins, and the observed and calculated masses of BthTx-I$^{1\text{-}7}$ and BthTx-I$^{101\text{-}107}$ show excellent agreement for all mutant proteins. The tryptic mutant peptides were also submitted to ESI–CID–MS/MS, and the deduced amino acid sequences shown in Table 1 unequivocally demonstrated the presence of the desired mutants.

The secondary structure of the purified recombinant protein was evaluated by far-UV CD, and as presented in Figure 1(A), both the native and the recombinant BthTx-I displayed minima at 209 and 222 nm, which indicates a predominantly α-helical secondary-structure content. These results are similar to those reported previously for BthTx-I [14,21,28], and confirm that the recombinant protein retains a total secondary-structure content similar to that found in the native protein. Figure 1(A) also shows that the L106F and L5F/V102A/L106F mutants show far-UV CD spectra that are very similar to those of the native protein purified from the snake venom and native recombinant protein. As shown in Figure 1(D), the ellipticity ratio for the minima at 222 and 209 nm ($\theta_{222}/\theta_{209}$) is close to unity for these four proteins. Figure 1(B) presents the far-UV CD spectra of the L106A and L5F/L106F mutants, which display significantly altered profiles, demonstrating that the secondary structure is significantly perturbed in these proteins. As shown in Figure 3, both these mutants displayed a myotoxic activity significantly different from that of the negative control, demonstrating that the loss of native protein structure is accompanied by loss of biological activity. However, Figures 1(C) and 1(D) show that the L5F, V102A, L5F/V102A and V102A/L106F mutants present slightly decreased values for the minimum at 209 nm in relation to the minimum at 222 nm. Although these differences are subtle, this observation suggests that, in these cases, mutagenesis in the hydrophobic core region results in perturbations of the secondary structure of the refolding protein.

The effect of mutagenesis in the substrate-binding region on the thermal denaturation curves was determined by monitoring the changes in the far-UV CD signal at 222 nm, and the fraction of unfolded protein f_u for each mutant as a function of temperature is presented in Figure 2. Estimates for the melting temperature T_m of the proteins can be derived from these denaturation curves, and as shown in Figure 2 (inset), the native, native recombinant and most of the mutant proteins show T_m values in the range 333–337 K. These results demonstrate that for most of the mutants tested, any structural change produced by site-directed mutagenesis did not significantly alter the thermal stability of the refolded proteins. However, as seen in Figure 2, the L5F and V102A/L106F mutants present reduced T_m values in the range 325–327 K. Comparison of the T_m results with the $\theta_{222}/\theta_{209}$ ratios (Figure 1D) shows that these two mutants present the greatest perturbations from the native far-UV CD spectra.

To evaluate the functional consequences of mutagenesis of the substrate-binding region, myotoxic activities of all these mutants were evaluated and the results are presented in Figure 3. As reported previously, the native and native recombinant proteins present identical myotoxic activities, suggesting that the recombinant protein has a completely conserved myotoxic determinant. The single-mutant L106F and the L5F/V102A/L106F mutant, which present far-UV CD spectra that are indistinguishable from the native protein, both show myotoxic activity equal to that of the native and wild-type recombinant proteins. In contrast, the single mutant V102A and the double mutants L5F/V102A and V102A/L106F show approx. 80 % of the activity observed for the native protein (significant at the $P < 0.05$ level), and the single mutant L5F shows approx. 60 % of the native protein activity. Comparison of these activities with the far-UV CD data presented in

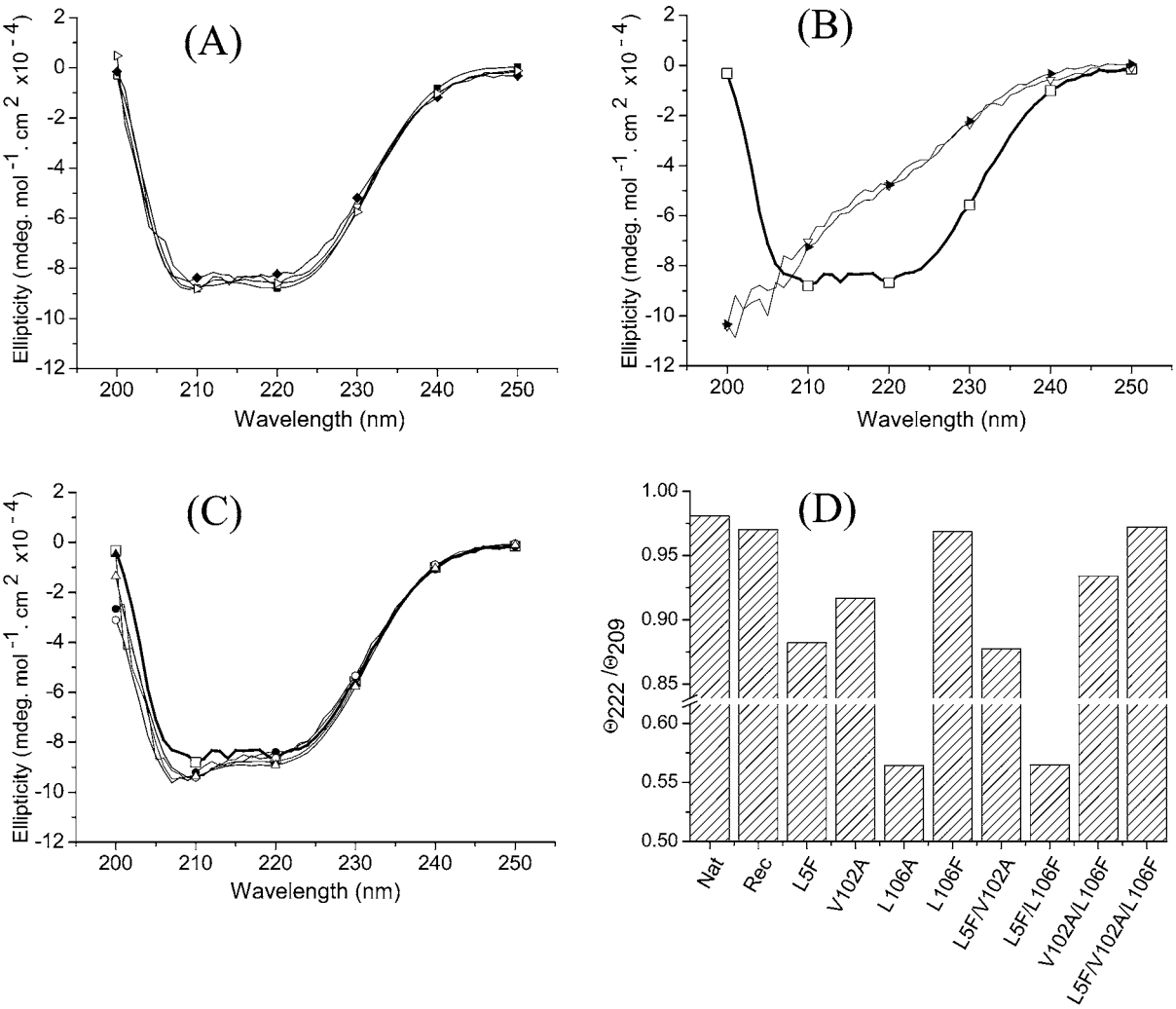

Figure 1 Far-UV CD spectra of native and recombinant BthTx-I after refolding and purification

(**A**) The native BthTx-I purified from *B. jararacussu* venom (■), the wild-type recombinant BthTx-I (□) and the mutants L106F (◆) and L5F/V102A/L106F (△). (**B**) Wild-type recombinant BthTx-I (thick solid line, □) and the mutants L106A (▽) and L5F/L106F (▲). (**C**) Wild-type recombinant BthTx-I (thick solid line, □) and the mutants L5F (●), V102A (▲), L5F/V102A (○) and V102A/L106F (△). (**D**) Ratio of the observed ellipticity signals at 222 and 209 nm for native BthTx-I (Nat), wild-type recombinant BthTx-I (Rec) and substrate-binding region mutants.

Figure 1(B) shows a striking correlation: those mutants in which an altered secondary structure is observed show decreased biological activity. Furthermore, the reduction in the biological activity is proportional to the perturbation of secondary structure, which suggests that myotoxic activity is a sensitive and reliable criterion to evaluate the structural effects of site-directed mutagenesis in the substrate-binding region.

Results of the myotoxic activity tests were compared with the results from the fluorescent marker release experiments (see Figure 4), and as reported previously, the native and native recombinant proteins were found to show similar levels of membrane-damaging activity [14,21,28]. The L106A and L5F/L106F mutants, which show a little or no myotoxic activity, also present significantly reduced levels of membrane-damaging activity, which is in accord with the loss of secondary structure observed with these proteins. Reduced levels of membrane-damaging activity are observed for the L5F and V102A mutants; this correlates well with the decrease in biological activity (see Figure 3) and supports the suggestion that these mutants have suffered conformational changes that result in the loss of protein function. The mutant L106F shows a level of membrane-damaging activity that is indistinguishable from the native protein, which is consistent with the full biological activity observed for this protein. However, for the L5F/V102A, V102A/L106F and the L5F/V102A/L106F mutants, there is no correlation between the myotoxic and membrane-damaging activities. The L5P/V102A mutant shows full membrane-damaging activity and a slightly reduced myotoxic activity, whereas the other two mutants show significantly reduced membrane-damaging activities even though the myotoxic activity is fully conserved (for the L5F/V102A/L106Fe mutant) or is only slightly decreased (for the V102A/L106F mutant). It has previously been demonstrated that the homodimer is the membrane-active form of the native BthTx-I [19]; therefore, the observed decrease in membrane-damaging activities of these mutants might be the consequence of altered dimer formation. This possibility was examined by measuring the hydrodynamic radius (R_h) by dynamic light scattering, which revealed that the native and wild-type recombinant proteins and all mutant proteins had an R_h value in the range 1.8–2.1 nm. These values are consistent with previously reported R_h values for the BthTx-I homodimer in solution

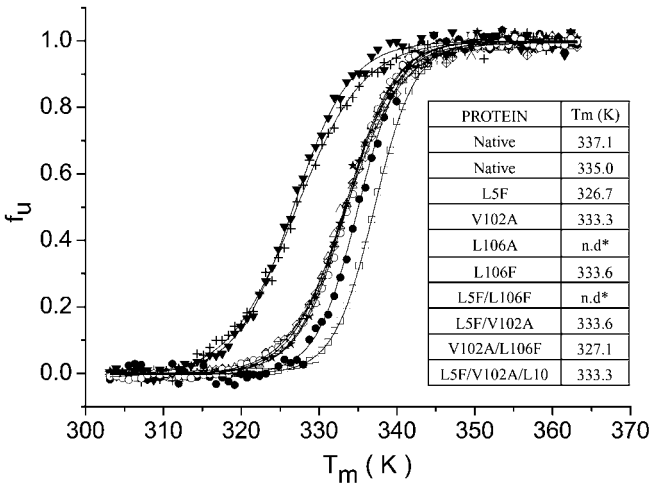

Figure 2 Fraction of unfolded protein f_u as a function of temperature for BthTx-I and substrate-binding region mutants

Native BthTx-I (□), wild-type recombinant BthTx-I (◆) and the mutants L5F (▼), V102A (●), L106F (○), L5F/V102A (crossed diamonds), V102A/L106F (+) and L5F/V102A/L106F (△). The inset presents the values of melting temperature T_m of BthTx-I before and after site-directed mutagenesis of residues in the substrate-binding region; n.d., value not determined.

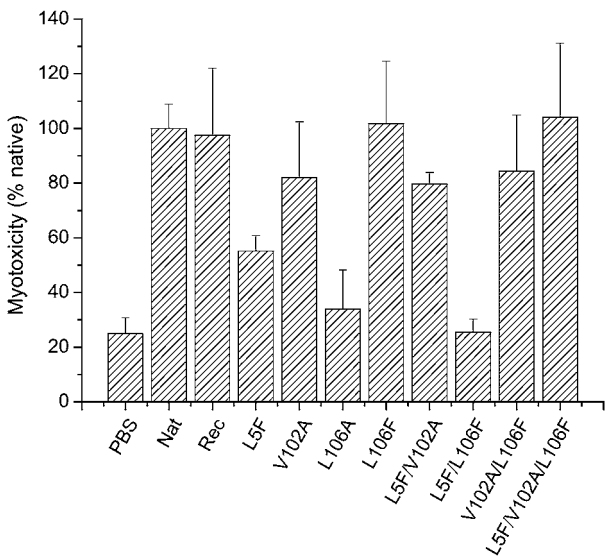

Figure 3 Plasma levels of CK activity 3 h after injection of 30 μg of native BthTx-I (Nat), wild-type recombinant BthTx-I (Rec) and substrate-binding site mutants into the gastrocnemius muscle of mice

The control experiment used an identical volume of PBS in the absence of protein. Results are expressed as the means ± S.D. for a minimum of five independent experiments.

[32], suggesting that the observed alterations in the membrane-damaging activities are not due to changes in the quaternary structure of the mutant proteins.

It has previously been reported that the Lys[49]-PLA_2s retain low levels of catalytic activity against 2-arachidonoyl-1-stearoyl-L-3-phosphatidylcholine [33,34], which raises the possibility that the altered active site of the Lys[49]-PLA_2s supports catalysis against a specific substrate. In this case, a specific topology of the substrate-binding region in the Lys[49]-PLA_2s may influence the orientation of the scissile ester bond of the substrate in the

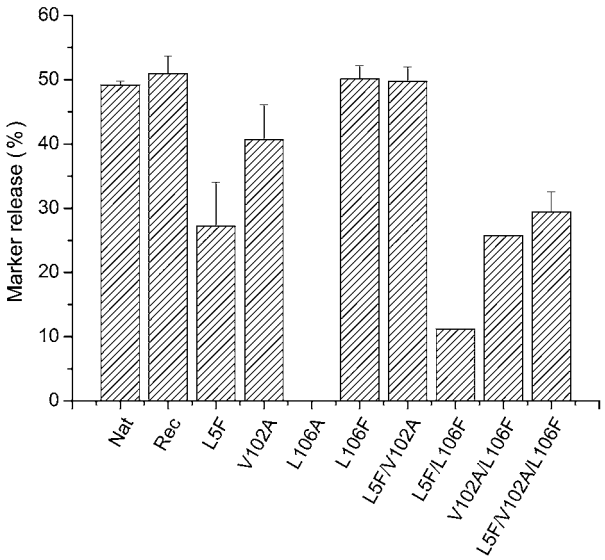

Figure 4 Release of entrapped calcein from liposomes composed of EYPC/DMPA at a 9:1 molar ratio 150 s after mixing with native BthTx-I (Nat), wild-type recombinant (Rec) and substrate-binding-site mutants at a protein/lipid ratio of 1:400

The final protein concentration in all experiments was 3 $\mu g \cdot ml^{-1}$, and the results are expressed as mean percentage of total calcein release after the addition of 5 mM Triton X-100.

active-site residues, thereby contributing to the specificity of the catalytic activity. Reversion of the topology of the substrate-binding region in the Lys[49]-PLA_2s to that found in the Asp[49]-PLA_2s might, therefore, result in reversion of the observed catalytic inactivation of Lys[49]-PLA_2s against mixed phospholipid substrates. However, catalytic activity tests with both the wild-type recombinant BthTx-I and the L5F/V102A/L106F mutant using a highly sensitive stopped flow Phenol Red assay [14] against either EYPC or 2-arachidonoyl-1-stearoyl-L-3-phosphatidylcholine substrates failed to detect substrate hydrolysis (results not shown). This result is in accord with the lack of detectable activity observed previously with recombinant BthTx-I [14] and supports the suggestion that the catalytic activity reported for the native Lys[49]-PLA_2 purified from snake venom is the result of trace contamination with catalytically active Asp[49]-PLA_2s.

DISCUSSION

The substrate-binding cleft and active-site residues for BthTx-I and the human-secreted class II Asp[49]-PLA_2 (hsPLA_2; PDB code 1BBC; [35]) are presented in Figures 5(A) and 5(B) respectively. The three residues at positions 5, 102 and 106 in the class I/II PLA_2s form a hydrophobic collar between the active-site region and the surface of the hydrophobic substrate-binding pocket. We have demonstrated previously that the Phe[5]/Ala[102]/Phe[106] cluster in hsPLA_2 and the Leu[5]/Val[102]/Leu[106] cluster in BthTx-I have combined volumes of 468.4 and 474.4 Å^3 respectively (1 Å = 0.1 nm) [22], and further analysis shows that the exposed hydrophobic surface areas are 27.5 and 22.3 Å^2 for the Phe[5]/Ala[102]/Phe[106] and Leu[5]/Val[102]/Leu[106] clusters respectively. In contrast with the conserved volumes and exposed surface areas, the atomic contacts between the three residues differ between Asp[49]-PLA_2 and Lys[49]-PLA_2. In the Asp[49]-PLA_2s, all residues in the Phe[5]/Ala[102]/Phe[106] cluster are in mutual contact; in contrast, in the Lys[49]-PLA_2s, side-chain

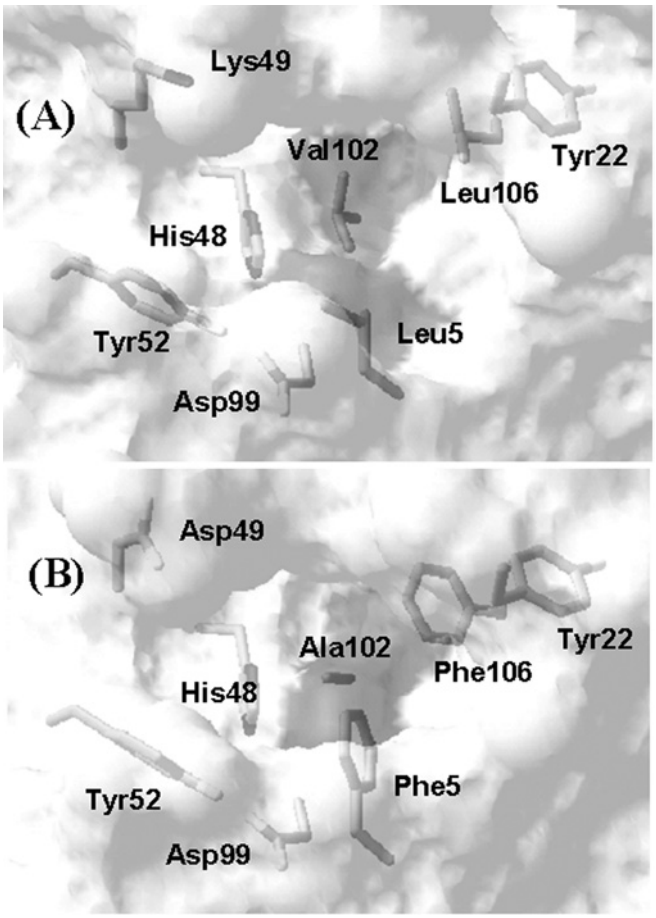

Figure 5 Transparent surface representation of the substrate-binding regions of (A) BthTx-I and (B) human group II secreted PLA_2 (PDB code 1BBC; [35]), showing the active-site (positions 48, 49, 52 and 99) and substrate-binding residues (positions 5, 22, 102 and 106) for both proteins

The solvent-accessible surface is shown, and the dark grey area in each Figure corresponds to the exposed surfaces of the side chains at positions 5, 102 and 106. The Figure was prepared using SwissPDB software [39].

contacts are formed between Val^{102} and Leu^{5} and between Val^{102} and Leu^{106}, but not between Leu^{5} and Leu^{106}. Furthermore, Figure 5 demonstrates that the specific amino acid substitutions at positions 5, 102 and 106 result in an altered topology of the substrate-binding region between Asp^{49}-PLA_2 and Lys^{49}-PLA_2, and the goal of the present study is to evaluate the effects of this change on the stability and Ca^{2+}-independent membrane-damaging activity of BthTx-I.

Mutagenesis of the substrate-binding region of BthTx-I influences both the conformation and stability of the protein, a clear indication that the packing of the hydrophobic core is of prime importance in conserving the native-like secondary and tertiary structures. The systematic approach adopted in the present study using single, double and triple mutants allows a comprehensive evaluation of the roles of side-chain packing in the substrate-binding region on the function of BthTx-I. As already noted, side-chain contacts in the Lys^{49}-PLA_2s are formed between Val^{102} and Leu^{5} and between Val^{102} and Leu^{106}, and although the mutation V102A reduces the side-chain volume at this position, the hydrophobic bridging contacts with Leu^{5} and Leu^{106} will be maintained. Therefore it could be expected that the structural alterations of this mutation would be minimized and, indeed, the far-UV CD spectra is only slightly perturbed and both the T_m value and the myotoxic activity are only slightly reduced with respect to the native protein.

Previous mutagenesis results with Asp^{49}-PLA_2s have demonstrated that a conserved hydrophobic volume at position 5 is essential for maintained levels of catalytic activity [25]. Superposition of the three-dimensional structures of BthTx-I and $hsPLA_2$ reveals that the introduction of an aromatic group at position 5 by the single-mutant L5F causes side-chain clashes with Val^{102}, and it is expected that structural reorganization of the substrate-binding region would be necessary to accommodate the introduction of the bulky aromatic ring. Although the single-mutant L5F refolds to a native-like structure with decreased myotoxic and membrane-damaging activities, the resulting protein has a low T_m value, which may reflect the structural perturbation in the hydrophobic core region. The packing conflict at position 5 is probably compounded by the additional substitution L106F and, indeed, the far-UV CD spectra demonstrate that the combination of these two mutations results in an unviable protein-refolding process. Conversely, mutations that reduce the side-chain packing problem at position 5 are more probable to favour protein refolding; thus a combination of V102A with L5F in L5F/V102A double mutant might reduce the side-chain clashes, and promote the observed gain in protein stability.

In the Asp^{49}-PLA_2s, aromatic stacking interactions are observed between the side chains of Tyr^{22} and Phe^{106}, and in the Lys^{49}-PLA_2s, the side chain of the Leu^{106} makes contact with the aromatic ring of the conserved Tyr^{22}. Thus, although the L106F mutant will increase the side-chain volume in the substrate-binding region, the mutant will introduce aromatic stacking interactions that may add to the stability of the contact between positions 22 and 106. Indeed, the L106F mutant retains native-like secondary structure and full myotoxic and membrane-damaging activities. These results with the Lys^{49}-PLA_2s are in broad agreement with those obtained from mutagenesis at the same positions in the Asp^{49}-PLA_2s, which demonstrated that single mutations at these positions that maintain the volume and hydrophobicity have minor effects on protein function [24]. This conclusion is supported by the loss of the ability of the L106A mutant in BthTx-I to refold to a native-like structure, emphasizing the importance of a maintained hydrophobic volume at this position. Side-chain packing also plays a role at position 106, and the reduced T_m value observed for the V102A/L106F mutant may be a consequence of the reduction in hydrophobic contacts caused by the reduction in the side-chain volume at position 102, a situation that is reverted by the completion of the hydrophobic packing by the mutation L5F in the L5F/V102A/L106F triad.

Thermal denaturation studies indicate that, in terms of stability, BthTx-I is surprisingly resilient to mutations in the substrate-binding cleft that result in the perturbation of the protein secondary structure. This may be attributed to the location of residues 5, 102 and 106 in the wall of the substrate-binding cleft, which may impart an enhanced plasticity to the packing interactions that would not be permitted for residues located deeper in the hydrophobic core of a protein. Thus alterations in the native secondary structure of BthTx-I that decrease the myotoxic and membrane-damaging activities may not decrease the thermal stability of the protein. When comparing the results of the structural studies with the changes in the Ca^{2+}-independent membrane-damaging activity after mutagenesis in the substrate-binding region, a key question is whether the effects on the membrane-damaging activity are the consequence of specific topology changes in the substrate-binding cleft rather than unspecific structural perturbations. Five substrate-binding site mutants of BthTx-I contribute to changes in the function that are coupled with alterations in the far-UV CD spectra (see Figures 1, 3 and 4), which we suggest are the

consequence of non-specific loss of the native-like protein structure. In contrast, two mutants contribute to changes in function that are not associated with changes in the far-UV CD spectra, which we suggest are probably the consequence of specific changes in the topology of the protein. Therefore, by comparing the myotoxic and membrane-damaging activities, the effects of specific and non-specific structural changes can be separated.

Both the far-UV CD spectrum and the myotoxic activity of L5F/V102A/L106F mutant are unaltered with respect to the native protein. If positions 5, 102 or 106 were direct structural determinants of the myotoxic effect, some effect of such extensive substitutions might be expected; therefore, the observed result suggests that the substrate-binding region is not a structural determinant of the myotoxic effect. This conclusion is in agreement with previous results that indicated that residues 116–122 in the C-terminal loop region directly participate in the determination of myotoxic activity [21]. Nevertheless, single and double mutations in the substrate-binding region result in a reduction of the myotoxic effect and the modification of the native-like protein structure, and the indirect effect of mutagenesis at positions 5, 102 and 106 suggest that a functional link exists between the substrate-binding and C-terminal loop regions of BthTx-I. Such a functional linkage explains the decreased myotoxic activity of Lys^{49}-PLA_2s after the modification of His^{48} in the active site by *p*-bromophenacyl bromide [36–38].

As for the case of the myotoxic effect, the results demonstrate that modification of the native-like structure resulting from mutagenesis in the substrate-binding region decreases the membrane-damaging activity. However, in contrast with the effects on myotoxicity, several mutants serve to demonstrate that structural changes in the substrate-binding region directly influence the membrane-damaging activity. This is clearly seen in the L5F/V102A/L106F mutant, which retains full myotoxicity, yet presents approx. 50 % of the membrane-damaging activity observed for the native and recombinant wild-type proteins. Previous mutagenesis studies have demonstrated that the C-terminal loop of BthTx-I is not only a myotoxic determinant, but is also involved in the Ca^{2+}-independent membrane-damaging activity [21], and the specific effects of mutagenesis in the substrate-binding region expand the known structural determinants of the calcium-independent membrane-damaging activity.

The question remains as to how topological changes in the substrate-binding region may influence the Ca^{2+}-independent membrane-damaging activity of the protein. The involvement of the substrate-binding region implies that, although substrate hydrolysis is not important, binding of phospholipid to the protein remains an important factor in the calcium-independent membrane-damaging process. Changes in the topology of the substrate-binding region may influence either the affinity of the substrate for the protein, the type of phospholipid that binds or the orientation of the bound lipid. In the present study, we have presented evidence supporting a functional linkage between the substrate-binding and C-terminal loop regions, which suggests that occupancy of the substrate-binding site may be a crucial event in the activity of the protein.

This work was partially supported by FAPESP (Fundação de Amparo à Pesquisa do Estado de São Paulo) grants 98/14569-3 (to J. M. S.), 98/14686-0 (to R. R.), 01/06388-3 (to T. L. F.), 00/11165-0 (to A. H. C. O.) and 96/11165-3 (to R. J. W.) and CNPq (Conselho Nacional De Desenvolvimento Científico e Tecnológico) grant 300725/98-1 (to R. J. W.).

REFERENCES

1 van Deenan, L. L. M. and de Haas, G. H. (1963) The substrate specificity of phospholipase A_2. Biochim. Biophys. Acta **70**, 538–553

2 Six, D. A. and Dennis, E. A. (2000) The expanding superfamily of phospholipase A(2) enzymes: classification and characterization. Biochim. Biophys. Acta **1488**, 1–19

3 Verheij, H. M., Volwerk, J. J., Jansen, E. H. J. M., Puyk, W. C., Dijkstra, B. W., Drenth, J. and de Haas, G. H. (1980) Methylation of histidine-48 in pancreatic phospholipase A_2. Role of histidine and calcium ion in the catalytic mechanism. Biochemistry **19**, 743–750

4 Scott, D. L., White, S. P., Otwinowski, Z., Yuan, W., Gelb, M. H. and Sigler, P. B. (1990) Interfacial catalysis: the mechanism of phospholipase A_2. Science **250**, 1541–1546

5 Gutierrez, J. M. and Lomonte, B. (1995) Phospholipase A_2 myotoxins from Bothrops snake venoms. Toxicon **33**, 1405–1424

6 Arni, R. K. and Ward, R. J. (1996) Phospholipase A_2 – a structural review. Toxicon **34**, 827–841

7 Ward, R. J., de Azevedo, Jr, W. F. and Arni, R. K. (1998) At the interface: crystal structures of phospholipases A_2. Toxicon **36**, 1623–1633

8 Maraganore, J. M., Merutka, G., Cho, W., Welches, W., Kezdy, F. J. and Heinrickson, R. L. (1984) A new class of phospholipase A_2 with lysine in place of aspartate 49. J. Biol. Chem. **259**, 13839–13843

9 Maraganore, J. M. and Heinrickson, R. L. (1986) The lysine-49 phospholipase A_2 from the venom of *Agkistrodon piscivorus piscivorus*. Relation of structure and function to other phospholipases A_2. J. Biol. Chem. **261**, 4797–4804

10 Homsi-Brandenburgo, M. I., Queiroz, L. S., Santo-Neto, H., Rodrigues-Simoni, L. and Giglio, J. R. (1988) Fractionation of *Bothrops jararacussu* snake venom: partial chemical characterization and biological activity of bothropstoxin. Toxicon **26**, 615–627

11 Condrea, E. (1989) Comparison of enzymatic and pharmacological activities of lysine-49 and aspartate-49 phospholipases A_2 from *Agkistrodon piscivorus piscivorus* snake venom. A reconsideration. Toxicon **27**, 705–706

12 Francis, B., Gutiérrez, J. M., Lomonte, B. and Kaiser, I. I. (1991) Myotoxin II from *Bothrops asper* (Terciopelo) venom is a lysine-49 phospholipase A_2. Arch. Biochem. Biophys. **284**, 352–359

13 Holland, D. R., Clancy, L. L., Muchmore, S. W., Rydel, T. J., Einspahr, H. M., Finzel, B. C., Heinrickson, R. L. and Watenpaugh, K. D. (1990) The crystal structure of a lysine 49 phospholipase A_2 from the venom of the cottonmouth snake at 2.0 Å resolution. J. Biol. Chem. **266**, 17649–17656

14 Ward, R. J., Chioato, L., de Oliveira, A. H. C., Ruller, R. and Sá, J. M. (2002) Active-site mutagenesis of a Lys^{49}-phospholipase A_2: biological and membrane-disrupting activities in the absence of catalysis. Biochem. J. **362**, 89–96

15 Arni, R. K., Ward, R. J., Gutiérrez, J. M. and Tulinsky, A. (1995) Structure of a calcium-independent phospholipase-like myotoxic protein from *Bothrops asper*. Acta Crystallogr. D **51**, 311–317

16 Scott, D. L., Achari, A., Vidal, J. C. and Sigler, P. B. (1992) Crystallographic and biochemical studies of the (inactive) Lys49 phospholipase A_2 from the venom of *Agkistrodon piscivorus piscivorus*. J. Biol. Chem. **267**, 22645–22657

17 Díaz, C., Gutiérrez, J. M., Lomonte, B. and Gene, J. A. (1991) The effect of myotoxins isolated from Bothrops snake venoms on multilamellar liposomes: relationship to phospholipase A_2, anticoagulant and myotoxic activities. Biochem. Biophys. Acta **1070**, 455–460

18 Rufini, S., Cesaroni, P., Desideri, R. F., Gubensek, F., Gutiérrez, J. M., Luly, P., Maassoud, R., Morero, R. and Pedersen, J. Z. (1992) Calcium ion independent membrane leakage induced by phospholipase-like myotoxins. Biochemistry **31**, 12424–12430

19 de Oliveira, A. H. C., Giglio, J. R., Andrião-Escarso, S. H., Ito, A. S. and Ward, R. J. (2001) A pH induced dissociation of the dimeric form of a lysine49 phospholipase A_2 abolishes Ca^{2+}-independent membrane damaging activity. Biochemistry **40**, 6912–6920

20 da Silva Giotto, M. T., Garratt, R. C., Oliva, G., Mascarenhas, Y. P., Giglio, J. R., Cintra, A. C., de Azevedo, Jr, W. F., Arni, R. K. and Ward, R. J. (1998) Crystallographic and spectroscopic characterization of a molecular hinge: conformational changes in bothropstoxin I, a dimeric Lys49-phospholipase A_2 homologue. Proteins **30**, 442–454

21 Chioato, L., de Oiveira, A. H. C., Ruller, R., Sá, J. M. and Ward, R. J. (2002) Distinct sites for myotoxic and membrane-damaging activities in the C-terminal region of a Lys49 phospholipase A_2. Biochem. J. **366**, 971–976

22 Ward, R. J., Rodrigues Alves, A., Rugierro Neto, J., Arni, R. K. and Casari, J. (1998) A SequenceSpace analysis of Lys49 phospholipases A_2: clues towards identification of residues involved in a novel mechanism of membrane damage and in myotoxicity. Protein Eng. **11**, 285–294

23 Maraganore, J. M., Merutka, G., Cho, W., Welches, W., Kezdy, F. J. and Heinrickson, R. L. (1984) A new class of phospholipase A_2 with lysine in place of aspartate 49. J. Biol. Chem. **259**, 13839–13843

24 Dupureur, C. M., Yu, B.-Z., Ramone, A., Jain, M. K. and Tsai, M.-D. (1992) Phospholipase A_2 engineering. The structural and functional roles of aromaticity and hydrophobicity in the conserved phenylalanine-22 and phenylalanine-106 aromatic sandwich. Biochemistry **31**, 10576–10583

25 Liu, X., Zhu, H., Huang, B., Rogers, J., Yu, B.-Z., Kumar, A., Jain, M. K., Sundaralingham, M. and Tsai, M.-D. (1995) Phospholipase A_2 engineering: probing the structural and functional roles of N-terminal residues with site-directed mutagenesis, X-ray, and NMR. Biochemistry **34**, 7322–7334
26 Homsi-Brandenburgo, M. I., Queiroz, L. S., Santo-Neto, H., Rodrigues-Simoni, L. and Giglio, J. R. (1988) Fractionation of *Bothrops jararacussu* snake venom: partial chemical characterization and biological activity of bothropstoxin. Toxicon **26**, 615–627
27 Ward, R. J., Monesi, N., Arni, R. K., Larson, R. E. and Paço-Larson, M. L. (1995) Sequence of a cDNA encoding bothropstoxin I, a myotoxin from the venom of *Bothrops jararacussu*. Gene **156**, 305–306
28 Ward, R. J., de Oliveira, A. H., Bortoleto, R. K., Rosa, J. C., Faca, V. M. and Greene, L. J. (2001) Refolding and purification of Bothropstoxin-I, a Lys49-phospholipase A_2 homologue, expressed as inclusion bodies in *Escherichia coli*. Protein Expr. Purif. **21**, 134–140
29 Heinrickson, R. L. (1991) Dissection and sequence analysis of phospholipase A_2. Methods Enzymol. **197**, 201–215
30 Nelson, M. R. and Long, G. L. (1989) A general method of site-specific mutagenesis using a modification of the Thermus aquaticus polymerase chain reaction. Anal. Biochem. **180**, 147–151
31 Yadav, S. and Ahmad, F. (2000) A new method for the determination of stability parameters of proteins from their heat-induced denaturation curves. Anal. Biochem. **283**, 207–213
32 Ruller, R., Ferreira, T. L., de Oliveira, A. H. C. and Ward, R. J. (2003) Chemical denaturation of a homodimeric lysine-49 phospholipase A_2: a stable dimer interface and a native monomeric intermediate. Arch. Biochem. Biophys. **411**, 112–120
33 Shimohigashi, Y., Tani, A., Matsumoto, H., Nakashima, K. and Yamaguchi, Y. (1995) Lysine-49-phospholipases A_2 from *Trimeresurus flavoviridis* venom are membrane-acting enzymes. J. Biochem. (Tokyo) **118**, 1037–1044
34 Yamaguchi, Y., Shimohigashi, Y., Chiwata, T., Tani, A., Chijiwa, T., Lomonte, B. and Ohno, M. (1997) Lys-49-phospholipases A_2 as active enzyme for β-arachidonoyl phospholipid bilayer membranes. Biochem. Mol. Biol. Int. **43**, 19–26
35 Wery, P., Schevitz, R. W., Clawson, D. K., Bobbitt, J. L., Dow, E. R., Gamboa, G., Goodson, T., Hermann, R. B., Kramer, R. M., McClure, D. B. et al. (1991) Structure of recombinant human rheumatoid arthritic synovial fluid phospholipase A_2 at 2.2 Å. Nature (London) **352**, 79–86
36 Diaz, C., Gutiérrez, J. M., Lomonte, B. and Nunez, L. (1993) *p*-Bromophenacyl bromide modification of *Bothrops asper* myotoxin II, a lysine-49 phospholipase A_2, affects its pharmacological activities. Toxicon **31**, 1202–1206
37 Andrião-Escarso, S. H., Soares, A. M., Rodrigues, V. M., Ângulo, Y., Diaz, C., Lomonte, B., Gutierrez, J. M. and Giglio, J. R. (2000) Myotoxic phospholipases A(2) in Bothrops snake venoms: effect of chemical modifications on the enzymatic and pharmacological properties of bothropstoxins from *Bothrops jararacussu*. Biochimie **82**, 755–763
38 Soares, A. M., Andrião-Escarso, S. H., Bortoleto, R. K., Rodrigues-Simioni, L., Arni, R. K., Ward, R. J., Gutierrez, J. M. and Giglio, J. R. (2001) Dissociation of enzymatic and pharmacological properties of piratoxins-I and -III, two myotoxic phospholipases A_2 from *Bothrops pirajai* snake venom. Arch. Biochem. Biophys. **387**, 188–196
39 Guex, N. and Peitsch, M. C. (1997) SWISS-MODEL and the Swiss-Pdb viewer: an environment for comparative protein modeling. Electrophoresis **18**, 2714–2723

Received 18 December 2003/11 May 2004; accepted 17 May 2004
Published as BJ Immediate Publication 17 May 2004, DOI 10.1042/BJ20031946